ICES Journal of Marine Science, 2022, **79**, 1075–1082
DOI: 10.1093/icesjms/fsac024
Advance access publication date: 18 February 2022
Original Article

Seasonal temperature regulates network connectivity of salmon louse

M. B. O. Huserbråten and I. A. Johnsen

Institute of Marine Research, Department of Oceanography and Climate, Bergen, Norway

* *Corresponding author: tel: +47 40482888; e-mail:* mats.huserbraaten@hi.no

Chronically high infestation of salmon louse (*Lepeophtheirus salmonis*) questions the sustainability of the Norwegian Atlantic salmon (*Salmo salar*) aquaculture industry. The confinement of millions of hosts, within hundreds of farms with overlapping larval dispersal kernels create the structure for extremely persistent parasite meta-populations. However, the processes regulating the temporal variation in cross-contamination of pelagic salmon louse stages among farms (i.e. connectivity), a vital process driving louse population dynamics, are not well described. Here, we employ a data driven biophysical dispersal model that reproduces three-and-a-half years of production histories of 132 salmon farms in western Norway and quantifies the connectivity of infective pelagic lice stages among the farms with the ocean currents. We show that although the complex geography of western Norwegian fjords governs the long-term topology of the connectivity network, there was a strong seasonal component to network fragmentation. The main de-structuring agent was the delayed infectivity of the pelagic lice stages at cooler temperatures increasing dispersal distances, enhanced by occasional large scale wind forcing events. Coordinated fallowing strategies and de-lousing treatments only played a marginal role in network fragmentation, suggesting that novel lice restraining strategies that consider the environmentally sensitive transport distances must be developed to successfully break up the connectivity network.

Keywords: aquaculture, biophysical modelling, connectivity, sea lice.

Introduction

Parasitic sea lice (Copepoda, Caligidae) are a growing economic problem to aquaculture worldwide due to their pathogenic effect on farmed bony fishes (Costello, 2006, 2009). Salmon louse (*Lepeophtheirus salmonis*) is the most commercially detrimental sea louse in the Northeast Atlantic, primarily due to its pathogenic effect on farmed Atlantic salmon (*Salmo salar*) produced in excess of 1.75 million tonnes annually (Iversen *et al.*, 2020). In Norway (the largest salmon producer worldwide) salmon louse related expenses average 9% of revenue, where the major costs include administration of pesticides, reduced marketability and growth, and increased stress to fish host (Abolofia *et al.*, 2017). The confinement of up to several million salmon hosts in relatively small cages, themselves often spaced well within the pelagic larval dispersal distance of the lice, creates a near-perfect template for an exponential growth of farmed lice meta-populations. Although salmon lice are natural parasites on wild populations of salmon, the infection pressure around a single farm can be more than 70 times greater than ambient levels, with elevated concentrations at distances up to 30 km (Krkošek *et al.*, 2005). This proliferation of farmed salmon louse in the natural habitat has drastic negative effects on wild salmon post-smolt, including lowered condition and increased mortality (Krkošek *et al.*, 2007; Johnsen *et al.*, 2020). In an effort to curb the negative effects of salmon lice farming on the wild salmonoid populations (primarily on Atlantic salmon, but also sea trout *Salmo trutta* and Arctic charr *Salvelinus alpinus*), the Norwegian aquaculture industry is currently governed by set mortality limits on wild salmon post-smolt migrating through the fjords, with independent/scientific bi-annual evaluations in 13 production zones (PZs) along the Norwegian coast. Most recent evaluations indicates that industry-induced mortality was acceptable (<10%) in nine PZs, moderate (10–30%) in two PZs, while two PZs had excessive mortality (>30%) (Vollset *et al.*, 2019).

The Hardangerfjord production zone (PZ3) is currently among the PZs where industry-induced mortality on wild post-smolt was estimated to be on moderate to high levels (>10%), and thus measures must be taken to reduce post-smolt mortality for future growth. PZ3 has a licensed production of up to 112.098 tonnes distributed among 132 farmed locations, and is home to several unique, wild salmon populations (Harvey *et al.*, 2019). The current management regime is based on a set limit of 0.5 adult salmon louse per fish, or 0.2 during post-smolt migration period in spring, reported weekly based on a random sample of 20 fish from every other cage at all farms. Moreover, to reduce cross-contamination of pelagic salmon lice and other infectious agents to newly stocked farms there are four coordinated stocking periods across a two-year period (spring, summer, odd and even years), preceded by at least two months of fallowing. This under the assumptions that a temporally and spatially staggered stocking scheme will reduce initial louse infestations, by limiting interactions (i.e. water contact) with farms containing a more mature louse demography (e.g. Bron *et al.*, 1993). The circulation of upper water masses in the Hardangerfjord system, where most of the pelagic life stages of the parasite is found (Heuch *et al.*, 1995), is mainly driven by large scale wind forcing and density fluctuations of the coastal water carried northwards by the Norwegian Coastal Current (NCC) (Asplin *et al.*, 2020; Dalsøren *et al.*, 2020). Due to high freshwater runoff into the fjords a brackish layer is often apparent in the upper 5–10 m, and the surface layer has a net outward flow (Figure 1).

Received: June 10, 2021. **Revised:** January 21, 2022. **Accepted:** January 31, 2022

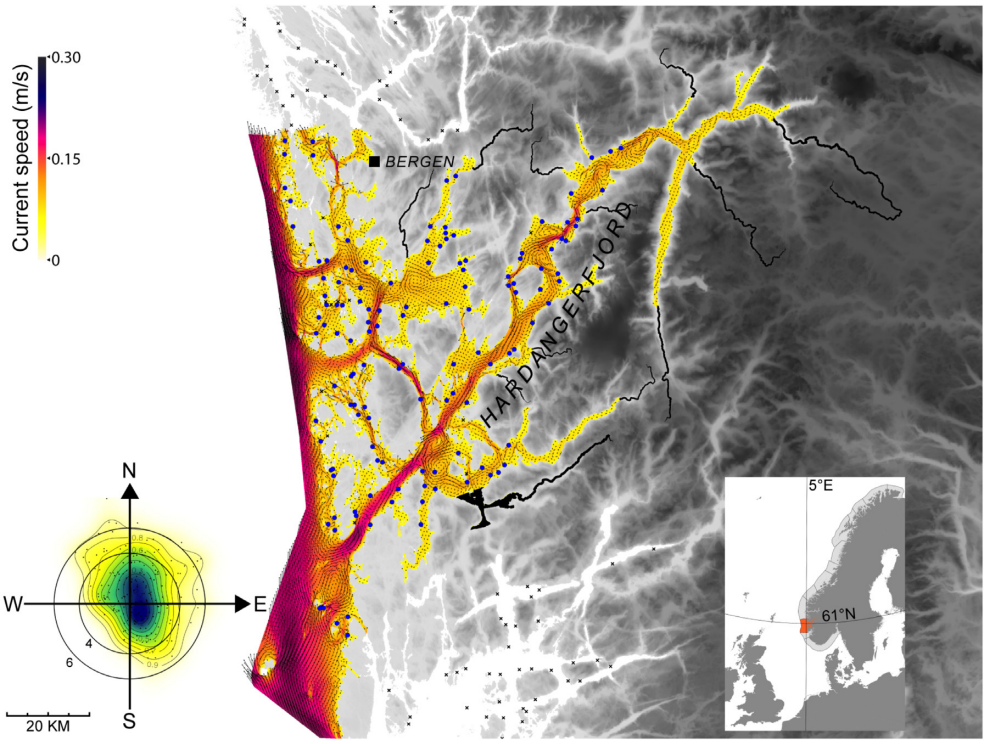

Figure 1. Overview of salmon farms (blue dots) in greater Hardangerfjord production zone (PZ3), and average modelled currents at 5 m over the three-and-a-half-year study period (yellow, orange, purple gradient). Also plotted is the sea-surface wind density function based on weekly averages (yellow, green, blue gradient), and 12 most important rivers for wild salmon populations in PZ3 (black lines).

From a network perspective (e.g. Barthélemy, 2011; Pastor-Satorras *et al.*, 2015) it is to be expected that decreasing the diversity of connections to upstream farms (in relation to flow of ocean currents) will reduce the external infestation pressure of salmon lice, decreasing the need for expensive and stressful treatments. Previous modelling works have addressed the external infestation pressure and network connectivity patterns by kernel density estimations (Kristoffersen *et al.*, 2014; Aldrin *et al.*, 2017; Cantrell *et al.*, 2018) and coupled ocean model and particle tracking algorithms (Adams *et al.*, 2016; Samsing *et al.*, 2017; Cantrell *et al.*, 2020). However, few studies have addressed the temporal dynamics of such a marine parasite network in detail. Here we apply a biophysical dispersal model that recreates the weekly connectivity patterns of pelagic salmon lice among farms over a three-and-a-half-year study period (1 April 2017 to 30 September 2020); with the overarching aim of: (i) quantifying the degree to which salmon farms in PZ3 are connected to each other via dispersal of louse pelagic stages (i.e. describe the long term network structure); and (ii) to quantify the variation in network structure through the seasons. Subsequently we wanted to explore several working hypotheses with regards to the drivers of variation in network fragmentation by evaluating the explanatory value of mixed effect models. Specifically we aimed to: (i) explore how louse physiological response to environmental factors could influence network fragmentation, for example through the temperature sensitive infectivity of louse as shown in laboratory studies (Skern-Mauritzen *et al.*, 2020); (ii) quantify how variation in large scale physical forcing could affect network fragmentation, for example by increasing/decreasing lice dispersal distances as suggested by Asplin *et al.* (2014); and finally, (iii) to test if the temporally and spatially staggered stocking scheme employed by the regional managers breaks up the network in any meaningful way, an important precondition to minimize transfer of pathogens between operational management units (e.g. Werkman *et al.*, 2011).

Materials and methods

Biophysical dispersal model

The hydrodynamic model used to represent the ocean currents, temperature, and salinity in the study area was based on the Regional Ocean Modeling System (ROMS, http://myroms.org), a free-surface, hydrostatic, primitive equations, general ocean circulation model (Shchepetkin & McWilliams, 2005). ROMS was run with a horizontal resolution of 160 × 160 m in an orthogonal, curvilinear grid covering the entire PZ3. The model was run with 35 vertical layers of depth-varying spacing (meaning tighter spacing/higher resolution at shallower depths) and with an increased resolution towards the surface. Hydrodynamic forcing on the model boundaries was applied from the larger NorKyst800 covering the entire Norwegian coast (see Albretsen *et al.*, 2011 for details); wind forcing was applied from the 2.5 km AROME-MetCoOp atmospheric model (Müller *et al.*, 2017); and daily freshwater discharge from the ∼170 rivers in the study area was provided by the Norwegian Directorate for Water Resources and Energy–all assembled hereafter referred to as the "NorFjords-setup" (see Asplin *et al.*, 2020 and Dalsøren *et al.*, 2020 for elaboration model on performance). The model was forced over the time period 1 April 2017 to 30 September 2020 with internal time steps of 6 s. The output from the NorFjords-setup contained velocity, salinity, and temperature fields with a temporal res-

olution of 1 h, thus adequately resolving the important tidal forces in the study area.

The advection of particles in the horizontal plane was modelled by the Runge–Kutta second order scheme "LADiM" with a random horizontal diffusion of up to 0.2 m^2/s (Ådlandsvik, 2020), evaluated every 2 min of the simulation period yielding a total of 920.880 time steps. At the same discrete time steps the vertical movement of pelagic salmon lice stages was evaluated, where particles were moved towards the surface when the light level exceeded a critical level, or downwards if salinity was lower than 31% (see detailed review and specific parameters used for lice behaviour in Sandvik *et al.*, 2020). One particle was released from each of the 132 farmed localities in PZ3 every hour of the study period, yielding 4.051.872 particles released in total.

To realistically represent the magnitude of dispersal of pelagic lice stages among the salmon farms while at the same time maintaining computational feasibility, each particle released in the model represented the predicted egg production at the farm (i.e. a super-particle; Scheffer *et al.*, 1995). Here, we integrated egg production at the farm level over the hourly release step as a function of incubation duration and temperature (see caption of Figure 2 in Stien *et al.*, 2005), average number of adult female lice at each farm (as reported to the Norwegian Food Safety Authority), with an assumption of two egg-strings per adult female carrying 150 eggs each (see results section in Stien *et al.*, 2005). After release, the super-particles experienced a fixed daily mortality of 0.17 (see results section in Stien *et al.*, 2005).

Network analyses

If super-particles drifted within a 160 m radius around farms (i.e. within nine grid cells in the hydrodynamic model) a proportion of the infective lice that the super-particles represented settled within the farm, dependent on age (in degree-days) and temperature experienced by the super-particle (equation [1] in Skern-Mauritzen *et al.*, 2020, and see Figure S1). Every week we integrated the number of modelled infective pelagic salmon lice originating from farm 1 infecting farm 2, 3, 4 … 132, and from farm 2 infecting farm 1, 3, 4 … 132 etc. The weekly integrated number of infective salmon lice exchanged among farms was stored in a 132∗132 matrix, for every 175 weeks of the study period, hereby referred to as "the connectivity matrix." To quantify the long term structure as well as seasonal variation in network fragmentation, we evaluated the community structure of the connectivity matrix both integrated over the entire study period and on a weekly basis. Here we used three different algorithms implementing very different approaches to detecting community structure, all available in R-package "igraph" (Csárdi & Nepusz, 2006). First and foremost, we used the "infomap" algorithm that minimizes the expected description length of a random walker trajectory within the connectivity matrix, both on the directed and undirected graph (Rosvall & Bergstrom, 2008); second, the "leading eigen-vector" method that tries to find densely connected subgraphs in a graph, by calculating the leading non-negative eigenvector of the modularity matrix of the graph (Newman, 2006); and third the "fast, greedy" method that tries to find dense subgraphs via directly optimizing a modularity score (Clauset *et al.*, 2004). The modularity score is an inherent property of a specific division of a graph, where a "good" division (corresponding to a low modularity score) generally have many edges within communities and only a few between them. Practically speaking, infomap's clusters are heuristically determined by the local retention rate of simulated random walkers within subdivisions guided by the weighted connectivity matrix links; while the eigenvector and greedy algorithms are pure mathematical constructions, by either dividing the modularity matrix (a mathematical derivation of the connectivity matrix) into clusters via eigenvalue spectral partitioning, or by directly minimizing the modularity score of different graph partitions, respectively. Due to the more intuitive design of the infomap algorithm the main results were viewed considering the communities found by infomap on the undirectional graph (as this implementation seemed least complex), but where apparent differences among the four programmatic iterations were discussed accordingly.

Linear modelling and variation partitioning

To quantify the effect of louse physiology, variation in natural environment, and management action on the temporal dynamics of the connectivity network, here measured as the median number of communities detected by the four clustering algorithms, we fitted mixed effect models to each predictor that hypothetically could be correlated based on prior knowledge (as outlined in introduction). The predictors tested (in total 15) could be classified into three general categories relating to either physiological response of lice to the environment, direct physical effects, or measures taken by management to reduce overall infestation pressure.

The six predictors related to management were (integrated over all farms belonging to PZ3): (i) trailing number of delousing treatments the previous four weeks; (ii) total number of fallowed farms; (iii) total standing mass of salmon reported for a given week; and number of fallowed farms following each of four different coordinated fallowing strategies, stocking the farms either in (iv) spring of even years, (v) summer in even years, (vi) spring in odd years, or (vii) summer in odd years. Determining which farm that belonged to either of the four fallowing strategies was based on a hierarchical cluster analysis on the similarity in production histories (i.e. weekly presence/absence of fish in farms). The cluster analyses were run with $k = 5$ groups, that allowed a fifth and separate group for farms that followed a sporadic fallowing regime (i.e. sporadic fallowing).

In total we tested the explanatory value of six physical variables, including: (i) current speed at 5 m (the average drift depth of pelagic lice); (ii) wind speed at sea surface (iii); wind speed of the south-north and east-west component (iv–v); and (vi) total freshwater discharge from all 178 rivers in the study area. All the physical variables were interpolated to the geographical grid of NorFjords-setup (including wind speed and direction extracted from the atmospheric model), averaged to weekly values, and only grid cells inside PZ3 and inshore of the national baseline was used.

The first (of two) physiological predictors tested was age at peak probability of infection, where infection probability of pelagic salmon louse was calculated as function of accumulated degree-days and temperature (cf. equation [1] in Skern-Mauritzen *et al.*, 2020, and Figure S1) through all drift trajectories. Subsequently the number of days (since hatch) until reaching peak probability of infection was identified for all particles. The second physiological predictor tested was drift depth as response to light and salinity (cf. Sandvik *et al.*, 2020). Both of these "in drift" physiological predictors were weekly

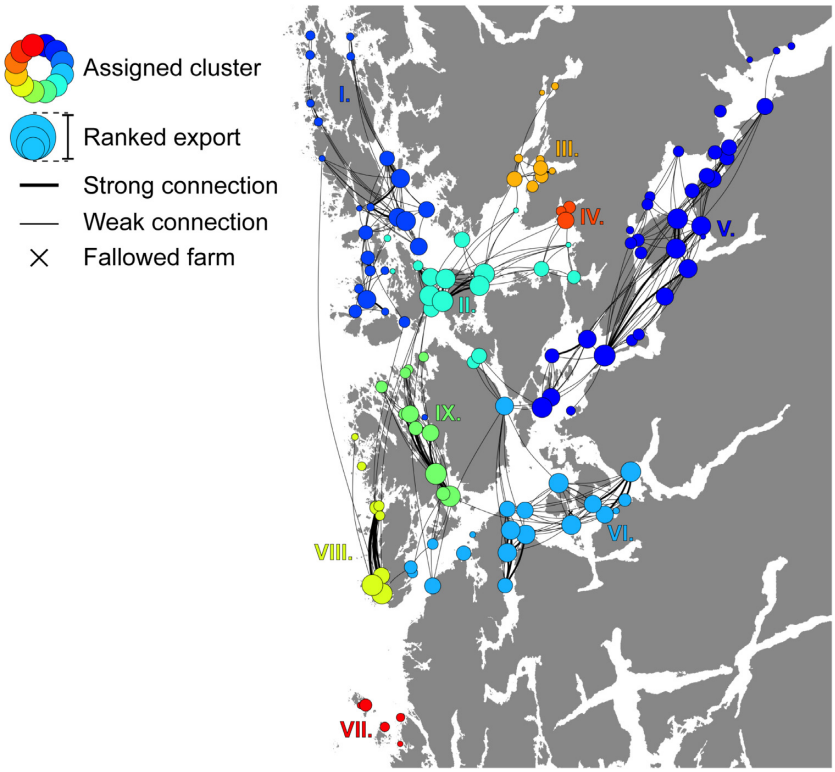

Figure 2. Community structure of PZ3 connectivity network, integrated over the three-and-a-half-year study period. Denoted with roman numerals 1–9 in a clockwise fashion are clusters: (I.) Øygarden-Austevoll, (II.) Bjørnafjord-Langnuen, (III.) Fusa-Eikeland-Samnangerfjord, (IV.) Sævareidsfjord, (V.) Hardanger-Kvinnheradsfjord, (VI.) Ål-Bjoa-Skåneviksfjord, (VII.) Haugesund, (VIII.) Bømlo, and (IX.) Fitjar-Stokksund. Arced connections between farms (black lines) represents the shortest path between farms (in a clockwise direction) and does not reflect the actual drift routes taken during model simulations. For clarity only the 500 strongest connections are plotted (represented by thin arcing lines), with thick arcing lines representing the 100 strongest connections.

averages of all individuals hatching/being released in a given week.

Explanatory power of the 15 models fitted was evaluated by the Akaike information criterion (AIC), an objective trade-off routine that balances goodness of fit and simplicity of the model (for the general idea for model selection criteria see Hastie & Pregibon, 2017). The AIC-evaluation was done in concurrence with the outcome from Likelihood-ratio tests (with cut-off at the 0.05 significance level), that assesses the goodness of fit of the two competing statistical models based on the ratio of their likelihoods. Subsequently, to explore the potential effect of an additional predictor, all the variables were again added to the top model from the first round and compared to the AIC of the top model of the first round. Moreover, as our response variable was measured at regular (weekly) time intervals they were not expected to strictly comply with assumptions of independence. Thus temporal autocorrelation of the residuals was accounted for using an auto-regressive model of order one. All model fitting was performed using the generalized least squares (gls) function in R library "linear and nonlinear mixed effects models"/"nlme" (Pinheiro *et al.*, 2021).

Results

Integrated over the entire study period, infomap revealed nine communities from the unidirectional graph (Figure 2). These nine communities of highly connected farms aligned well with the major topographical features of the region, for example distinguishing large clusters in the Hardangerfjord (V., *cf.* Figure 2), and the Skåneviksfjord (VI.). Infomap also distinguished lesser topographically constrained communities, for example along the Austevoll/Øygarden archipelago (I.), and in the Bjørnafjord (II.). On a general basis, three of the four community detection algorithms (the two infomap implementations and the fast and greedy method) converged on almost identical partitions of the long-term graph (Figure S2).

Although the long-term topology of the network followed the large-scale geographical features, the network varied considerably on a weekly basis, for example from no fragmentation in January 2018, to up to 11 communities in July 2019 (Figure 3).

On closer inspection there was a clear seasonal variability in network fragmentation as suggested by all four community detection algorithms (Figure 4A), where the median weekly number of communities identified had a negative correlation with number of connections ($cor_{Nclust\ vs.\ Nconn} = -0.61$, $t = -10.1$, $df = 173$, $p<0.001$). In total, three of the mixed effects models constructed showed explanatory power on median weekly number of communities, as evaluated by a combination of reduced AIC (compared to the null model) and significant p-values from the Likelihood ratio tests (Table 1). As was clear based on model AIC, the first and by far the most important predictor in explaining variation in network fragmentation was age of peak infectivity, which in turn was highly correlated with temperature ($cor_{Temp\ vs.\ Infect} = -0.94$, $t = -36.01$, $df = 173$, $p<0.001$, Figure 4B); where a delayed infectivity of pelagic stages associated with lower temperature

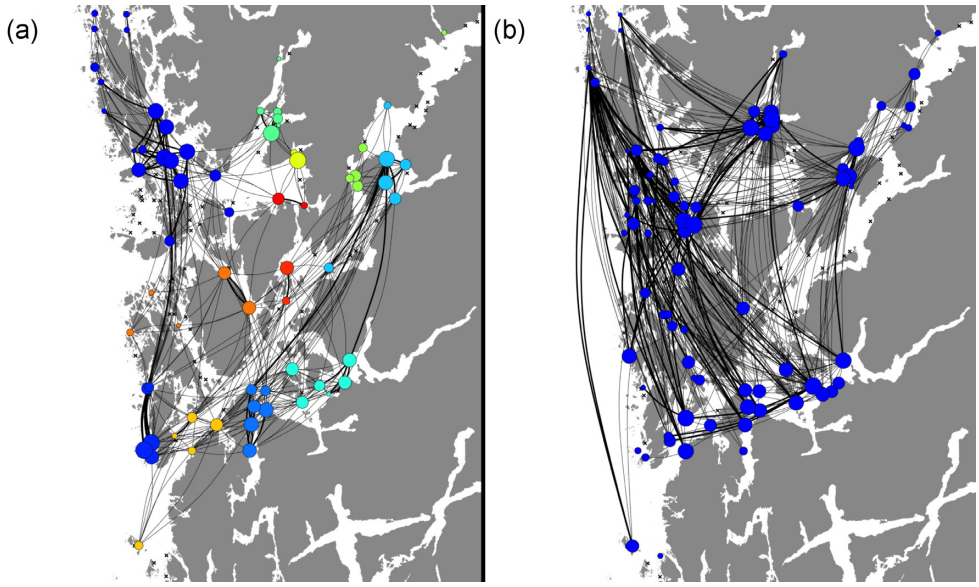

Figure 3. Connectivity networks of pelagic salmon lice stages among farm localities in PZ3, with contrasts of two weekly integrated connectivity networks: (**A**) highly fragmented network with localities partitioned into 11 clusters (week 33, 2019), and (**B**) an unfragmented network with (week 4, 2018). For further figure descriptions, see Figure 2.

corresponded to a decreased fragmentation. The second most important predictor was increased wind anomalies from the south (meaning high positive S to N deviations) co-occurring with low fragmentation (Figure 4C). The top mixed effect model fitted (with regards to lowest AIC), combining age of peak infectivity and S-N wind anomalies, had an pseudo-R^2 (i.e. correlation between predicted and observed number of communities) of 0.73 (see Table 2 for top-model estimated parameters, and Table S1 for all fitted model parameters). However, note that the correlation structure between age of peak infectivity and S-N wind anomalies in the mixed effect model was estimated to –0.14, indicating some degree of (negative) co-variability between the two variables. Temporal autocorrelation of residuals was estimated to 0.38, meaning that network fragmentation one week out had a correlation of 0.38, two weeks out 0.38^2 (= 0.14) etc. Overall, there were no systematic deviations between model predictions and observed fragmentation over time, indicating that the combination of the two predictors could adequately represent most of the processes that created the seasonal pattern in network fragmentation (Figure 4E).

Discussion

While the topographically steered circulation pattern of the western Norwegian fjords constrains the long-term structure of the connectivity network, the main driver of variation in fragmentation through the season was time until onset of peak infectivity of louse, directly mediated by the seasonal temperature. However, the co-variability of seasonal temperature and large-scale wind forcing confounds the interpretation of the results to some degree. For example, along-fjord internal waves forced by S-N wind episodes are most frequent in winter and spring and advects a substantial amount of lice along the Hardangerfjord (Asplin *et al.*, 2014); while at the same time the low temperatures in winter delays peak infectivity by several weeks (Skern-Mauritzen *et al.*, 2020), increasing the potential for dispersal drastically. Moreover, a central parameter that needs to be optimized in community detection applications on large networks is modularity (e.g. Clauset *et al.*, 2004; Newman, 2006). Three of the four community detection algorithms applied in our analyses implement some form of optimization on modularity (only infomap on the directional graph omits this step), and three of the resulting long-term partitions were highly correlated, although with the eigenvector method deviating substantially from the other three. Comparing our long term graph (i.e. Figure 2) with the findings of Samsing *et al.* (2017) using the eigenvector method; we find a large discrepancy between our nine communities, and Samsing's two communities within the same area. Other differences in approach was that the time integration periods were different between our studies (two seasons in Samsing *et al.*, 2017 vs. inter-annual integration in Figure 2), age and temperature dependent infectivity was not implemented (cf. Skern-Mauritzen *et al.*, 2020), and the hydrodynamical model resolution used was different (800 m vs. 160 m, although otherwise using very similar configurations). Thus future, high(er)-resolution studies on a nation-wide scale are needed to resolve these apparent incongruences in community detection.

Management action through the regional fallowing scheme had an almost negligible effect on network fragmentation. Bron *et al.* (1993) reported strong effect of fallowing on a farm-level by reducing infestation pressure during the initial stocking phase. Yet simple deterministic models suggests that for synchronized fallowing to be most effective in isolating the newly stocked farms, long-distance connections into the management unit has to be reduced substantially (Werkman *et al.*, 2011; Murray & Salama, 2016). The persistently high external infestation pressure typical within the densely farmed PZ3 most likely decreases the network "fragmentation effect" of fallowing to a large extent (Guarracino *et al.*, 2018). Corollary, if operational fallowing units were optimally divided, as for example suggested by community detection algorithms that explicitly minimize the interconnectivity across communities, we predict that external infestation pressure during the

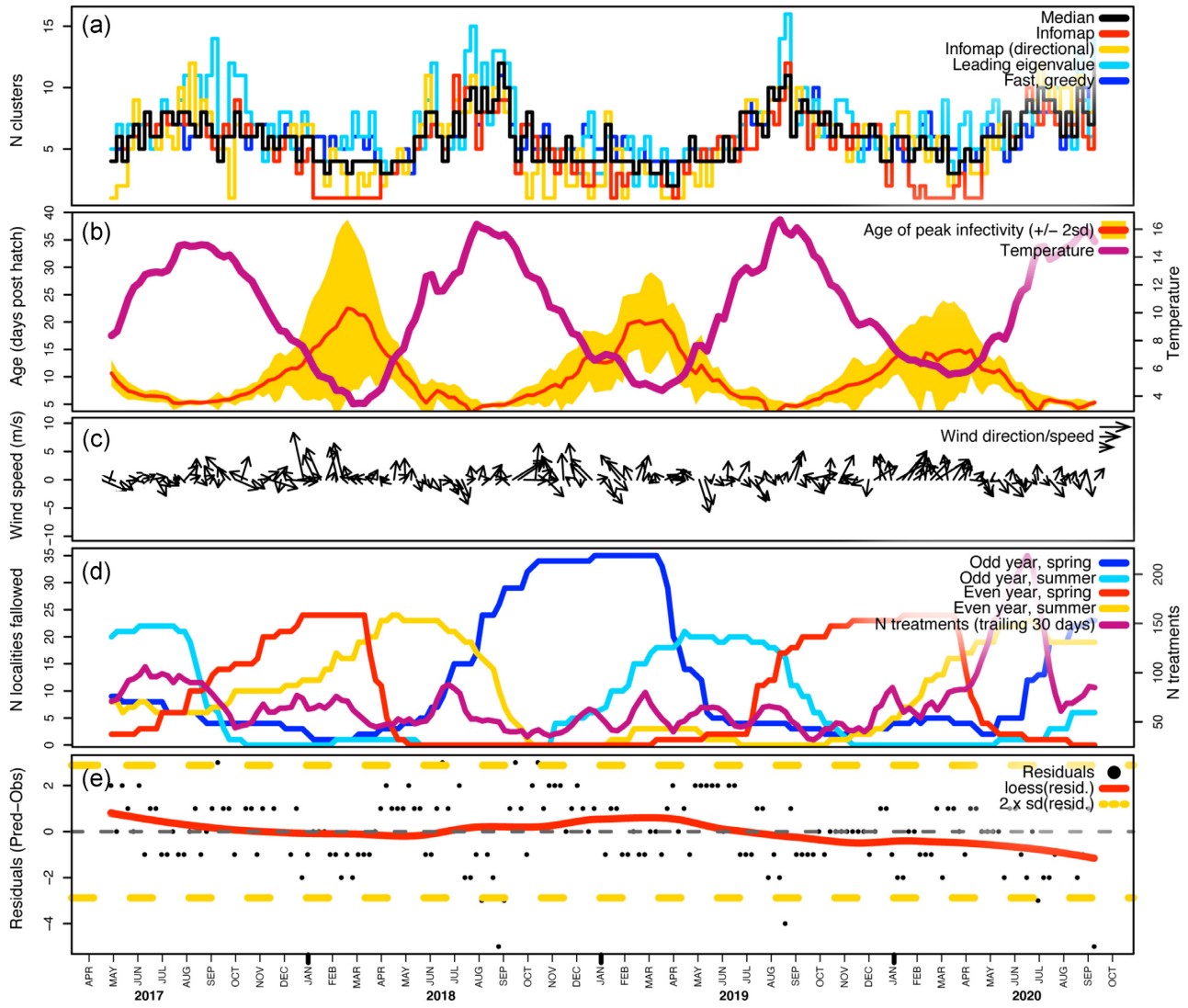

Figure 4. Time series of response variable and predictors tested during model selection: (a) number of communities identified by the four different community detection algorithms and their combined median; (b) age of peak infectivity (in days post hatch) of pelagic lice stages and "in-silico" temperature of lice at drift; (c) prevalent wind direction and speed on sea-surface averaged over the study area, where cardinal direction of arrows indicates wind direction (i.e. arrows pointing upwards means winds generally blowing from the south) and length of arrows indicates speed; (d) number of fallowed localities during four main coordinated stocking strategies and number of trailing (30-days) treatments; and (e) residuals of the top mixed effects model (including predictors age of peak infectivity and S-N wind anomalies) plotted over the weeks of the study period.

Table 1. Results from the two-step model selection procedure presenting all mixed effect models that showed increased explanatory power compared to the null-model, as evaluated by a decrease in AIC. However, do note that in model selection round 1 models 1.1–1.5 are compared to model 0, while in round 2 models 2.1–2.6 are compared to model 1.1. Also presented is model AIC (and difference in AIC when comparing models, Delta AIC), log-Likelihood of the model, the likelihood ratio between respective models, and *p*-values from likelihood ratio tests comparing the models.

Model	Predictor	AIC	Delta AIC	logLik	L-Ratio	*p*-value
0	NULL	641.94	-	-317.97	-	-
1.1	**+peakage**	**602.50**	**-39.44**	**-297.25**	**41.44**	**0.000**
1.2	+northavg	633.58	-8.36	-312.79	10.36	0.001
1.3	+mass	640.28	-1.67	-316.14	3.67	0.056
1.4	+Fallow2	640.74	-1.20	-316.37	3.20	0.074
1.5	+currentavg	640.98	-0.96	-316.49	2.96	0.085
2.1	**peakage + northavg**	**597.33**	**-5.17**	**-293.67**	**7.17**	**0.007**
2.2	peakage + currentavg	601.07	-1.43	-295.54	3.43	0.064
2.3	peakage + Fallow4	601.66	-0.84	-295.83	2.84	0.092
2.4	peakage + ntreat	601.95	-0.55	-295.98	2.55	0.110
2.5	peakage + Fallow2	602.16	-0.34	-296.08	2.34	0.126
2.6	peakage + mass	602.22	-0.29	-296.11	2.29	0.130

Table 2. Estimated parameters from the top mixed effects model (as evaluated by lowest AIC), fitted to predictors age of peak infectivity and S-N wind anomalies (model 2.1 in Table 1).

Predictor	Parameter estimate	Std.Error	t-value	*p*-value
(Intercept)	8.85	0.36	24.92	0.000
peakage	-0.29	0.03	-8.85	0.000
northavg	-0.11	0.04	-2.72	0.007

initial stocking phase could be drastically reduced; in turn scaling down the need for expensive and stressful/harmful delousing treatments. However, further explorations into new fallowing strategies are needed, for example by employing a fully dynamical meta-population model (as opposed to a data-driven model used here), simulating fallowing and stocking at different times allowing one to break up the statistical dependencies inherent to this correlative study.

Although this study was performed in PZ3, a seasonality in network fragmentation is probably also typical in other areas–yet most likely less pronounced and with larger communities at higher latitudes due to lower average temperatures. Similarly, in accordance to future climate warming scenarios (e.g. Sandvik *et al.*, 2021) we generally predict a higher fragmentation. However, further studies are needed to make plausible projections of future warming on network fragmentation, where a regional downscaling of future warming scenarios have to be implemented directly into the biophysical dispersal simulations.

To conclude, we observed a highly structured connectivity network of salmon louse in the Hardangerfjord area, where the main de-structuring agent was the seasonally oscillating temperature lengthening/shortening pelagic larval durations by up to several weeks. However, this seasonal pattern was occasionally disrupted by large scale wind events, at times strong enough to unify the entire PZ infestation network into one highly connected unit. At the other extreme we observed high fragmentation during the summer months, when temperatures were high and disruptive large scale circulation events were rare. Furthermore, management action through the historical fallowing regime of PZ3 had no observable effect on network fragmentation. Although detailed suggestions for novel fallowing strategies may be premature based on this correlative study, we argue that the connectivity is generally too high among the operational management units for fallowing to have a noticeable effect on network fragmentation. On a general basis, we thus recommend larger operational fallowing units on a scale similar to the communities of our long-term network (i.e. on a fjord scale, *viz.* Figure 2); where the fixed topology of the PZ may play a greater role in fragmenting the network, and thus increase the overall effectiveness of fallowing.

Supplementary Data

Supplementary material is available at the *ICESJMS* online version of the manuscript.

Author contributions

M.B.O.H. performed the simulations and analyses, and wrote the main manuscript. I.A.J. participated in the development of the relevant research questions, and helped revise the manuscript.

Conflict of interest

The authors declare no conflict of interest.

Data availability

The data underlying this article will be shared on reasonable request to the corresponding author.

References

Abolofia, J., Wilen, J. E., and Asche, F. 2017. The cost of lice: quantifying the impacts of parasitic sea lice on farmed salmon. Marine Resource Economics, 32: 329–349.

Adams, T. P., Aleynik, D., and Black, K. D. 2016. Temporal variability in sea lice population connectivity and implications for regional management protocols. Aquaculture Environment Interactions, 8: 585–596.

Ådlandsvik, B. 2020. Lagrangian advection and diffusion model (LADiM). URL: https://github.com/bjornaa/ladim.

Albretsen, J., Sperrevik, A. K., Sandvik, A. D., and Asplin, L. 2011. NorKyst-800 report no. 1 user manual and technical descriptions. Fisk og Havet, 2: 1–48.

Aldrin, M., Huseby, R. B., Stien, A., Grøntvedt, R. N., Viljugrein, H., and Jansen, P. A. 2017. A stage-structured bayesian hierarchical model for salmon lice populations at individual salmon farms – estimated from multiple farm data sets. Ecological Modelling, 359: 333–348.

Asplin, L., Albretsen, J., Johnsen, I. A., and Sandvik, A. D. 2020. The hydrodynamic foundation for salmon lice dispersion modeling along the norwegian coast. Ocean Dynamics, 70: 1151–1167.

Asplin, L., Johnsen, I. A., Sandvik, A. D., Albretsen, J., Sundfjord, V., Aure, J., and Boxaspen, K. K. 2014. Dispersion of salmon lice in the hardangerfjord. Marine Biology Research, 10: 216–225.

Barthélemy, M. 2011. Spatial networks. Physics Reports, 499: 1–101.

Bron, J. E., Sommerville, C., Wootten, R., and Rae, G. H. 1993. Fallowing of marine atlantic salmon, salmo salar L., farms as a method for the control of sea lice, lepeophtheirus salmonis (Kroyer, 1837). Journal of Fish Diseases, 16: 487–493.

Cantrell, D., Filgueira, R., Revie, C. W., Rees, E. E., Vanderstichel, R., Guo, M., Foreman, M. G. G. *et al.* 2020. The relevance of larval biology on spatiotemporal patterns of pathogen connectivity among open-marine salmon farms. Canadian Journal of Fisheries and Aquatic Sciences, 77: 505–519.

Cantrell, D. L., Rees, E. E., Vanderstichel, R., Grant, J., Filgueira, R., and Revie, C. W. 2018. The use of kernel density estimation with a biophysical model provides a method to quantify connectivity among salmon farms: spatial planning and management with epidemiological relevance. Frontiers in Veterinary Science, 5: 1–14.

Clauset, A., Newman, M. E. J., and Moore, C. 2004. Finding community structure in very large networks. Phys Rev E - Stat Physics, Plasmas, Fluids, Relat Interdiscip Top, 70: 6.

Costello, M. J. 2006. Ecology of sea lice parasitic on farmed and wild fish. Trends in Parasitology, 22: 475–483.

Costello, M. J. 2009. The global economic cost of sea lice to the salmonid farming industry. Journal of Fish Diseases, 32: 115–118.

Csárdi, G., and Nepusz, T. 2006. The igraph software package for complex network research. Inter Journal Complex Sy, 1695.

Dalsøren, S., Albretsen, J., and Asplin, L. 2020. Estuarine, coastal and shelf science new validation method for hydrodynamic fjord models applied in the. Estuarine, Coastal and Shelf Science, 246: 107028.

Guarracino, M., Qviller, L., and Lillehaug, A. 2018. Evaluation of aquaculture management zones as a control measure for salmon lice in norway. Diseases of Aquatic Organisms, 130: 1–9.

Harvey, A. C., Quintela, M., Glover, K. A., Karlsen, N. R., Skaala, S. H., Kålås, S., Knutar, S. *et al.* 2019. Inferring atlantic salmon post-smolt migration patterns using genetic assignment. Royal Society Open Science, 6: 190426.

Hastie, T., and Pregibon, D. 2017. Routledge Generalized linear models. In Statistical Models in S, pp. 195–247

Heuch, P. A., Parsons, A., and Boxaspen, K. 1995. Diel vertical migration: a possible host-finding mechanism in salmon louse (Lepeophtheirus salmonis) copepodids? Canadian Journal of Fisheries and Aquatic Sciences, 52: 681–689.

Iversen, A., Asche, F., Hermansen, Ø., and Nystøyl, R. 2020. Production cost and competitiveness in major salmon farming countries 2003–2018. Aquaculture, 522: 735089.

Johnsen, I. A., Harvey, A., Sævik, P. N., Sandvik, A. D., Ugedal, O., Ådlandsvik, B., Wennevik, V. *et al.* 2020. Salmon lice-induced mortality of atlantic salmon during post-smolt migration in norway. ICES Journal of Marine Science,

Kristoffersen, A. B., Jimenez, D., Viljugrein, H., Grøntvedt, R., Stien, A., and Jansen, P. A. 2014. Large scale modelling of salmon lice (Lepeophtheirus salmonis) infection pressure based on lice monitoring data from norwegian salmonid farms. Epidemics, 9: 31–39.

Krkošek, M., Ford, J. S., Morton, A., Lele, S., Myers, R., and Lewis, M. 2007. Declining wild salmon populations in relation to parasites from farm salmon. Science, 318: 1772–1775.

Krkošek, M., Lewis, M. A., and Volpe, J. P. 2005. Transmission dynamics of parasitic sea lice from farm to wild salmon. Proceedings of the Royal Society B: Biological Sciences, 272: 689–696.

Müller, M., Homleid, M., Ivarsson, K. I., Køltzow, M. A. Ø., Lindskog, M., Midtbø, K. H., Andrae, U. *et al.* 2017. AROME-MetCoOp: a nordic convective-scale operational weather prediction model. Weather and Forecasting, 32: 609–627.

Murray, A. G., and Salama, N. K. G. 2016. A simple model of the role of area management in the control of sea lice. Ecological Modelling, 337: 39–47.

Newman, M. E. J. 2006. Finding community structure in networks using the eigenvectors of matrices. Physical Review E, 74.

Pastor-Satorras, R., Castellano, C., Van, M. P., and Vespignani, A. 2015. Epidemic processes in complex networks. Reviews of Modern Physics, 87: 925–979.

Pinheiro, J., Bates, D., Debroy, S., and Sarkar, D. 2021. nlme: linear and nonlinear mixed effects models.

Rosvall, M., and Bergstrom, C. T. 2008. Maps of random walks on complex networks reveal community structure. Proceedings of the National Academy of Sciences, 105: 1118–1123.

Samsing, F., Johnsen, I., Dempster, T., Oppedal, F., and Treml, E. A. 2017. Network analysis reveals strong seasonality in the dispersal of a marine parasite and identifies areas for coordinated management. Landscape Ecology, 32: 1953–1967.

Sandvik, A. D., Dalvin, S., Skern-mauritzen, R., and Skogen, M. D. 2021. The effect of a warmer climate on the salmon lice infection pressure from norwegian aquaculture. Ices Journal of Marine Science, 78: 1849–1859, doi:10.1093/icesjms/fsab069.

Sandvik, A. D., Johnsen, I. A., Myksvoll, M. S., Sævik, P. N., and Skogen, M. D. 2020. Prediction of the salmon lice infestation pressure in a norwegian fjord. Ices Journal of Marine Science, 77: 746–756.

Scheffer, M., Baveco, J. M., DeAngelis, D. L., Rose, K. A., and van Nes, E. H. 1995. Super-individuals a simple solution for modelling large populations on an individual basis. Ecological Modelling, 80: 161–170.

Shchepetkin, A. F., and McWilliams, J. C. 2005. The regional oceanic modeling system (ROMS): a split-explicit, free-surface, topography-following-coordinate oceanic model. Ocean Modelling, 9: 347–404.

Skern-Mauritzen, R., Sissener, N. H., Sandvik, A. D., Meier, S., Sævik, P. N., Skogen, M. D., Vågseth, T. *et al.* 2020. Parasite development affect dispersal dynamics; infectivity, activity and energetic status in cohorts of salmon louse copepodids. Journal of Experimental Marine Biology and Ecology, 530-531: 151429.

Stien, A., Bjørn, P. A., Heuch, P. A., and Elston, D. A. 2005. Population dynamics of salmon lice lepeophtheirus salmonis on atlantic salmon and sea trout. Marine Ecology Progress Series, 290: 263–275.

Vollset, K. W., Nilsen, F., Ellingsen, I., Finstad, B., Helgesen, K. O., Karlsen, Ø., Sandvik, A. D. *et al.* 2019. Vurdering av lakselusindusert villfiskdødelighet per produksjonsområde i 2019.

Werkman, M., Green, D. M., Murray, A. G., and Turnbull, J. F. 2011. The effectiveness of fallowing strategies in disease control in salmon aquaculture assessed with an SIS model. Preventive Veterinary Medicine, 98: 64–73.

Handling Editor: Carrie Byron